Archeologia e Calcolatori
30, 2019, 347-365

MULTISENSOR-MULTISCALE APPROACH IN STUDYING THE PROTO-HISTORIC SETTLEMENT OF BOSTEL IN NORTHERN ITALY

1. Introduction

Historical excavations in the proto-historic village of Bostel (Fig. 1), in the municipality of Rotzo (Vicenza, Italy), seem to indicate that the ancient village was way bigger than the public area of the archaeological park, which is the focus of all most recent field interventions. Since no ground-based excavations or geophysical surveys are allowed in the private fields surrounding the park, we opted for a remotely sensed approach using unmanned aerial vehicle (UAV) surveys and aerial/satellite imaging. In particular, the site was selected to evaluate a set of integrated methods for the cross-validation of data acquired from different sensors in order to improve the accuracy of photo-interpretation and decrease the number of false positives to be checked with field surveys or geophysical prospections, with reference to a ground truth validation protocol (Hoffer 1972; Steven 1987). Moreover, we tested a low-cost/high performance UAV prototype for archaeological applications and a consumer-level DJI Phantom 2 drone.

Since the early 2000s, UAVs are becoming a popular tool for archaeological prospection, with a real explosion of case studies and published papers in the last five years (Colomina, Molina 2014; Borie 2016; Parcero-Oubiña *et al.* 2016; Campana 2017 and cited bibliography). Their use covers a wide range of archaeological applications, from heritage mapping and monitoring to photogrammetry and acquisition of tridimensional data (e.g. Chiabrando *et al.* 2011; Fiorillo *et al.* 2013) and represents a harbinger research field, pointing to prominent developments in the next few years.

2. Archaeological context

The ancient settlement of Bostel was discovered back in 1781 by the local scholar Agostino Dal Pozzo, who suggested the presence of a village with more than six hundred houses (Dal Pozzo 1820). Scientific investigations resumed in 1912 with a short mission led by Giuseppe Pellegrini (1915-1916) that uncovered the so-called throne room, a longhouse with a ritual and/or public destination on the top of the promontory. In 1969, Giovanni Battista Frescura opened a series of trenches and identified the structures known as 'sector A' (Leonardi, Ruta Serafini 1981) and 'sector B' (Fig. 2). Since 1993, the University of Padova (Unipd) is conducting extensive archaeological

Fig. 1 – Location and overview of the Bostel promontory, in the municipality of Rotzo (province of Vicenza, Italy).

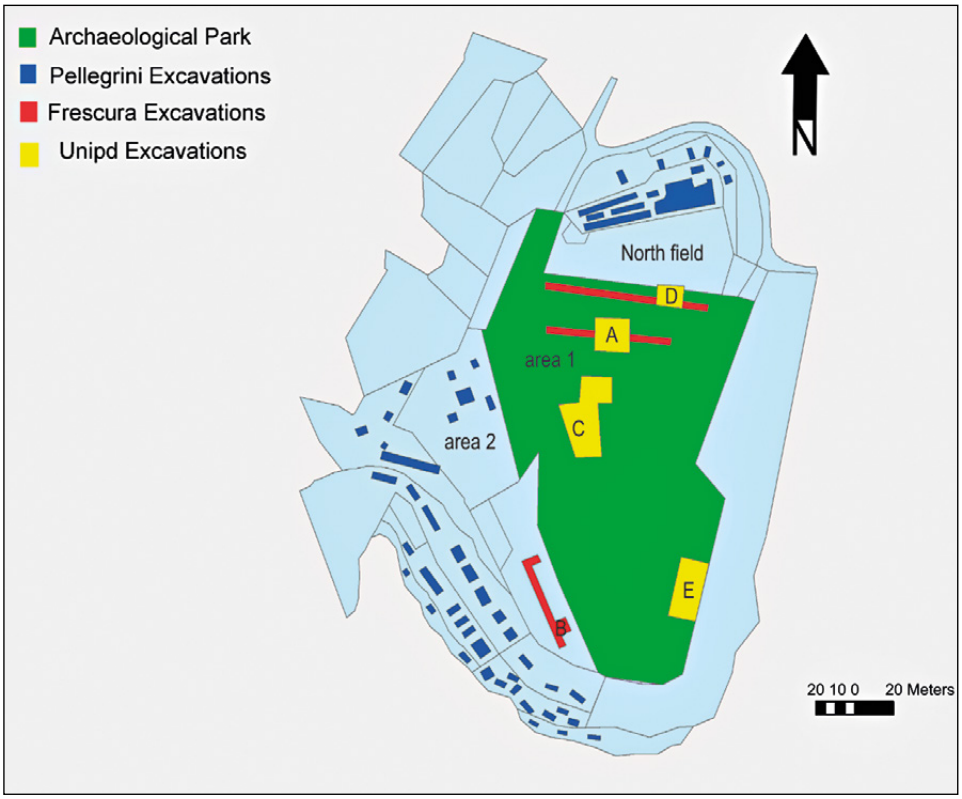

Fig. 2 – Location of the historical and contemporary excavations and trenches on the Bostel: in blue Pellegrini's excavations of 1912; in red Frescura's excavations of 1969; in yellow the excavations of the University of Padova (Unipd), 1993-ongoing. The area of the archaeological park (referred throughout the text as 'area 1') is highlighted in green.

investigations aimed at understanding the chronological sequence and the spatial organization of the settlement (De Guio *et al.* 2011). The most recent campaigns are focusing on the northern edge of the archaeological park, where a new house unit and a series of terraces were recently discovered in 'sector D' (Magnini *et al.* 2017a).

The village is located on a pre-alpine promontory controlling both the Assa and the Astico valleys. The study of the material culture, combined with the stratigraphic evidence, highlighted at least two main phases: sporadic traces of human frequentation date back to the Late Bronze Age/Early Iron Age (XII-VIII century BC), with no structural remains. The settlement was occupied during the Second Iron Age (V-II century BC) and until the Roman conquest of the area (De Guio *et al.* 2011). Only seven house units have been identified and excavated so far. They are semi-buried houses, traditionally associated with Raetic groups (Perini 1967; Migliavacca 1994). This kind of dwelling is characterized by a quadrangular perimeter in dry-stones associated to wooden walls and a roof in perishable material. There is no direct evidence of the coverage, while fragments of burnt wooden beams were recovered in limited cases.

Despite the rich bibliography related to the material culture and the building technologies of the central-eastern Alpine settlements in Northern Italy during the Second Iron Age (Lora, Ruta Serafini 1992; Migliavacca 1996; Marzatico 2001; Leonardi 2010 with references), few is known about the intra-site organization of the villages. In fact, most discoveries are related to emergency excavations which could identify and excavate only limited areas, often comprising one or few house units and their immediate surroundings (see e.g. Leonardi *et al.* 2011; Tecchiati, Sabattoli 2011; Tecchiati, Rizzi 2014; Solano 2016). Instead, the case of Bostel offers the opportunity to study a well-preserved context, with a potentially very high number of domestic structures and infrastructures.

3. Materials and methods

This work focuses on the identification of the structural and infrastructural organization of the Bostel village, with specific interest in the localization of new buried structures. According to what is known from recent and historical digs, the average dimension of the houses of the Bostel settlement ranges in the order of 25-40 m², similarly to what is known for other, coeval sites (Migliavacca 1996). The buildings related to breeding and food storing, could vary in size from several meters to ca. 50 cm. The same can be said for pathways, terrace walls and water channels (Pellegrini 1915-1916; De Guio *et al.* 2011; Magnini *et al.* 2017a). It should, however, be noticed that the post-depositional processes and the agricultural exploitation of the area

have partially altered the original, post-abandonment topography of the site, reducing the visibility of the micromorphological traces related to the Iron Age settlement (Magnini, Bettineschi 2019).

For this reason, we employed a multisensor protocol of increasing spatial resolution comprising satellite multispectral and panchromatic imaging coupled with aerial orthophotos and VHR (very high resolution) Digital Elevation Models (DEM) derived from UAV surveys. The detection limit of each technique will be better discussed in the dedicated sections.

3.1 *Octocopter prototype*

The HORUS octocopter drone (Colombatti *et al.* 2017) has been designed to provide an increased payload capacity and improved flight duration in comparison with the commercial available UAVs, reaching up to 30-40 minutes of flight time depending on the payload. The final configuration of the drone has been selected after a trade-off study taking into account ease

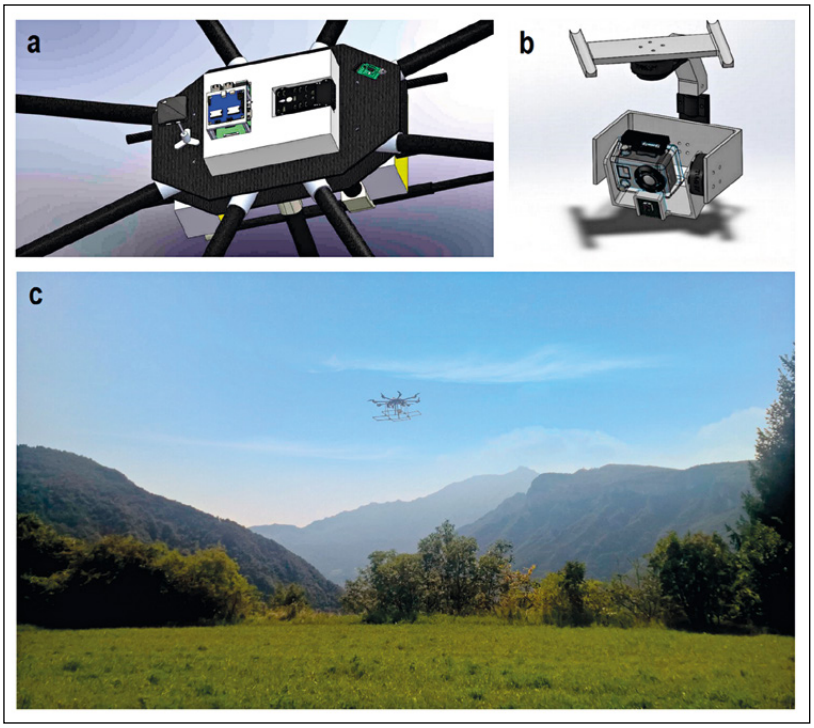

Fig. 3 – The HORUS octocopter prototype: a) CAD model detail of the upper section; b) CAD model of the gimbal subsystem; c) the octocopter during one of the flights above the Bostel.

of operations (take-off, flight and landing), low susceptibility to wind and turbulence during flight and repeatability in image capture quality.

The main structure is a foldable commercial structure in carbon fiber (Tarot T15), with a custom designed and 3D printed gimbal for hosting sensors (Fig. 3). The gimbal can be actively controlled on two or three axes using a SimpleBGC 32-bit card. The current-controlled brushless motors (Turnigy 4008) ensure a constant pointing direction towards the ground, regardless of the drone position.

Overall mass of the octocopter including all subsystems is around 8 kg with a maximum allowable payload mass of 4 kg. Flight operations are achieved by controlling eight rotor wings with 15' blades through a 3DR Pixhawk autopilot system; trajectory and attitude can be manually controlled or GPS guided and tracked to allow geo-referenced data acquisition.

Flight control algorithm verification was based on a drone model developed in Matlab's multibody software, SimMechanics. Through the modelling of actuators, controllers, and external forces, it was possible to investigate the stability of the drone under conditions of motion disturbance and to predict its behaviour and effectiveness in following trajectories. The validity of the model was then verified by conducting flight tests in a controlled area. The purpose of this test is to verify the system's ability not to deviate from the required position for an extended time span.

The octocopter is equipped with a GoPro Hero4 camera and a Flir Lepton thermal camera fixed on the gimbal structure. Correct nadir pointing of the VIS and IR cameras is controlled with a closed loop by a dedicated software implemented on an Arduino UNO architecture using inertial sensors for attitude determination. Images are acquired by a dedicated on-board Raspberry PI2 computer, tagged with drone timing and position data and then stored onboard for later analysis.

Power is provided by two lipo battery packs, able to guarantee an overall flight time slightly above 30 minutes.

3.2 *Available topographic data and UAV surveys*

The geographic data available for the municipality of Rotzo comprise various sets of grey scale or RGB aerial images from 1982 to 2010 (with spatial resolution up to 16 cm), historical cartography and modern maps issued by the Military Geographic Institute. The only morphological data available is a 5 m resolution topographic Digital Elevation Model (DEM), that is not sufficient for the recognition and identification of archaeological evidences at site and near-site or intra-site level (Fig. 4b).

In order to obtain higher resolution images and related 3D models of the Bostel promontory and its surroundings, we led several flights with a Phantom 2 commercial drone (equipped with a GoPro Hero 3 black edition) and our

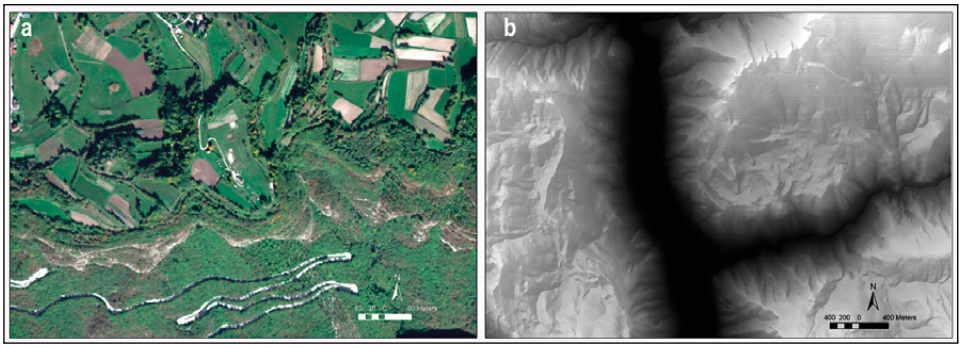

Fig. 4 – a) WorldView 2 8-band multispectral image (ground resolution 1.6 m); b) 5 m resolution topographic Digital Elevation Model of the Western Asiago Plateau (province of Vicenza, Italy).

custom HORUS octocopter. The cameras were set up to automatically shoot at regular intervals of two seconds. Data were acquired in different periods of the year and hours of the day; this allowed us to evaluate the variability of the soil and grass-marks in different seasons and select the most meaningful images for archaeological interpretations.

The flight altitude was derived from the resolution on the ground required for the images in the visible and infrared spectra. Having the sensors different resolutions, passages at different heights were required to ensure the same ground resolution. The flight altitude is obtained from:

$$H = \frac{D_{DSG}\, f}{d}$$

where D_{DSG} is the ground resolution (cm/pixel), H is the flight altitude, f is the focal distance, d is the size of the single pixel (He *et al.* 2012).

For example, the GoPro Hero 4 camera has a focal length of 2.77 mm, a 4000×3000 pixel matrix with a single pixel size of 0.001598 mm; the requirement of 0.5 cm/pixel resolution can be realized with a flying height of 8.7 meters. The field of view in both directions and the trajectory needed by the overlay required for subsequent processing was calculated accordingly. Data were acquired using manual remote-control flight and automated flight via waypoints grid at a height ranging according to the specific test from 8 to 15 m. The surveys resulted in more than 2400 images per image set.

3.3 *Structure from Motion-derived DEM*

The absence of LiDAR data for the municipality of Rotzo and the scarce vegetation canopy on the site, make the Bostel an ideal place for testing Structure from Motion (SfM). Structure from Motion is a Computer Vision

technique that offers the possibility to extract three-dimensional models from photographic datasets with an appropriate overlapping range (Green *et al.* 2014). Basically, SfM can automatically identify matching points in photographic shots taken from multiple directions around a scene, when a good degree of overlap between the different images is assured (Ma *et al.* 2001). The presence/absence and, subsequently, the position of these points are monitored through the sequence of multiple images. Using this information, it is possible to reconstruct a 3-dimensional model in the form of a sparse point cloud.

For generating the DEMs of the site, we used the software PhotoScan Professional 1.1.6 (Agisoft LLC) (Verhoeven 2011). 120 out of more than 2400 images were selected for generating a DEM with a 4 cm ground resolution covering the non-wooded area of the promontory (area 1). Although the use of a higher resolution digital model (up to 1 cm or less of spatial resolution) offers a better accuracy, in most cases the additional data are not only uninformative for archaeological purposes but they also represent a disturbing agent for the detection of meaningful surface anomalies. Grass blades or a sequence of tilled clods may provide a significant amount of noise especially when image enhancement treatments are applied. Furthermore, the choice of a lower resolution model is justified by the size of the anomalies to be identified and the need to obtain a smaller file for improved post-processing speed.

The subsequent accuracy assessment and the georeferencing of the 3D models were performed using a ground control points (GCP) reference set, recorded with a differential GPS LeicaCS10 and a total station Leica FlexLine TS06.

The same protocol was also applied to the creation of digital elevation models from close-range imagery. Sectors C1, C2 and D, which are currently under excavation, were mapped to document the progression of the works (Fig. 5), such as already proposed in the literature (i.e. De Reu *et al.* 2013; Benavides López *et al.* 2016).

3.4 *DEM visualisations and topographic analysis*

In recent years, the use of DEMs has significantly improved the identification, mapping and monitoring of archaeological sites and structures (Holden *et al.* 2002; Crutchley 2015; Kokalj, Hesse 2017; Magnini *et al.* 2017b; Burigana, Magnini 2018). The development of new techniques of data acquisition with different sensors, resolution, processing time and economical costs (such as SfM, photogrammetry, airborne laser scanning, stereo satellite imagery, radar interferometry etc.) provides the archaeologists with a wide selection of approaches to choose from, according to their specific historical questions.

However, a DEM does not represent the final product for archaeological photo-interpretation. In fact, the 3D model can be further processed to highlight ground anomalies possibly related to near-surface or sub-surface

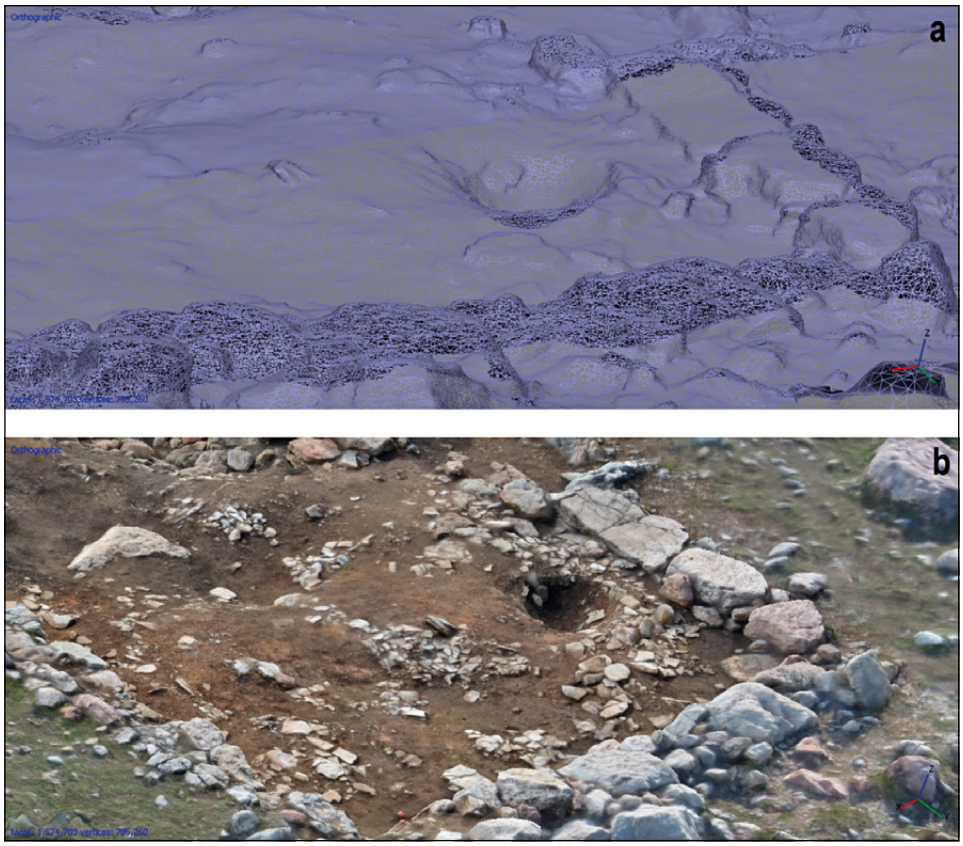

Fig. 5 – Sector C1, detail showing the perimetric walls of the house unit and the area of the pottery kilns. Structure from Motion data processing: a) wireframe mesh; b) textured multi-resolution 3D model.

structures. For the selection of the specific image enhancement methods, we took into account the different types of anomalies associated with the archaeological structures potentially present on the Bostel and we tested several visualization techniques to emphasize morphological variations linked to eventual archaeological features, using various commercial and open-source software (ArcGIS, LiVT, RVT, SAGA GIS).

The Hillshade is a visualization that generates an artificial illumination on a digital model; this visualization technique highlights anomalies illuminated obliquely with respect to the light source, but hides the parallel ones. To avoid this issue, we calculated the PCA of 16 different hillshades: this multivariate analysis summarizes the highest level of meaningful variance into a limited number of principal components. For archaeological purposes, it is a good

practice to check the secondary components that may also contain some crucial data for interpretation (Deveraux *et al.* 2008). Due to its versatility, the PCA can be applied on very different datasets, including images acquired from the same sensor or from different sources.

The Sky-View Factor (SVF) measures the portion of the visible sky from every point on the surface of the model. Its algorithm considers all physical objects that affect the visibility of the celestial hemisphere, firstly on the 180 degrees of the plane angle and secondly on 360 degrees of the solid angle (Zaksek *et al.* 2011). The raster output provides a non-dimensional parameter between 0 (obscured view) and 1 (clear view) (Kidd, Chapman 2012). The analysis of Slope highlights the gradient of a digital elevation model. It is calculated as the value of maximum elevation change between each cell of the grid and the adjacent ones (Challis *et al.* 2011). The use of the Flow Direction visualization technique is the key for the hydrological analysis of a surface. It calculates the direction of flow using the steepest descent from every cell in the raster. The output is a false colour image where the value of every cell represents the direction of the flow (Jenson, Domingue 1988).The ability of Local Relief Model (LRM) to highlight local elevation differences makes it one of the most powerful visualization tools for archaeological prospection. After removing landscape-level morphologies, this algorithm significantly increases the visibility of micro-morphologies, independently from the illumination angle (Hesse 2010).

3.5 *Multispectral imaging*

Whilst not densely forested, the Bostel has a thick grass coverage that serves as a surface mediator which can reveal, through its state of health (i.e. its greenness) the presence of buried structures altering the vegetation nourishment. In order to investigate this context, we chose to work with images from Worldwiew-2 satellite which provide a good compromise between spatial and spectral resolution, being equipped with 8 sensors in the visible to near infrared range (panchromatic ground resolution 40 cm; multispectral ground resolution 1.6 m) (Fig. 4a).

Digital colour images are normally displayed in a composition of three bands corresponding to the three additive primary colours: red layer/red band, green layer/green band and blue layer/blue band (RGB), respectively corresponding to Worldview bands 5, 3 and 2. Knowing the frequencies corresponding to the characteristic reflection of certain categories of objects, we can select three bands for RGB visualization in order to bring out a certain type of information, in our case the archaeological record. The most typical false colours composition includes near infrared 1 (NIR1, band 7), red and green; the effect is similar to the traditional false colour IR visualisation. It is a combination especially useful to observe the tree coverage and to monitor

the plant growth, which is conditioned by soil drainage properties, and thus can be altered in presence of buried structures or anthropic deposits. Two compositions particularly suitable for investigating mixed flora landscapes are those of bands 7, 6 and 5 (NIR1, red edge and red): these bands cover the sensitive portion of the spectrum corresponding to the transition from chlorophyll absorption to its reflection in plants. It is a combination particularly useful to identify small anomalies in the arboreal cover; band 7 (NIR1), 3 (green) and 2 (blue) composition is useful to differentiate the tone of coniferous, deciduous plants and grass cover. These two solutions have been successfully adopted for the area of Bostel of Rotzo.

The Decorrelation Stretch (or D-Stretch) is an algorithm generated as an extension of the PCA of multispectral data (Estornell *et al.* 2013). It is classified as a color enhancement algorithm as it accentuates the differences between each channel in the image (Gillespie *et al.* 1986). D-Stretch modifies the image by exasperating the less correlated color information; it is employed on a transformed image space and only at the end of the operating process the results are re-converted in RGB. The algorithm was applied to the 'natural colors' band set (bands 5, 3 and 2) but also, experimentally, on different band sets of Rotzo's Worldview-2 data.

In all cases, pansharpening algorithms were performed on the images before the decorrelation, to obtain a greater degree of spatial detail indispensable for an in-depth interpretation.

Other efficient image enhancing strategies for multispectral images involve the treatment of individual bands as algebraic terms (map algebra). Vegetation indices (or VIs) have been developed with the purpose of producing representative models of critical vegetation properties (De Guio 2015). The most popular among them is the Normalized Difference Vegetation Index or NDVI, a standard indicator that estimates the local biomass, or the amount of substance made up of vegetal organisms in relation to the surface (Lillesand *et al.* 2008):

$$NDVI = \frac{(NIR - Red)}{(NIR + Red)}$$

NDVI was implemented on Bostel multispectral image, along with two variants: *Green Normalized Difference Vegetation Index* (GNDVI), in which Red band is substituted by the Green one, and *Worldview Improved Vegetative Index* (WV-VI), that instead of conventional infrared uses NIR2 (860-1040 nm), a band introduced with the launch of Worldview-2 covering larger wavelengths and a wider spectral share of the spectrum. In addition to vegetation analysis, the multispectral data is suitable for calculating other types of indexes more focused on different properties of the scene. WorldView-2 Soil Index or WVSI (Wolf 2010) uses yellow and green bands to identify spatial units in the landscape and thus the pixels in the image mostly consisting in soil:

$$WVSI = \frac{(Green - Yellow)}{(Green + Yellow)}$$

The Normalized Difference Mud Index or NDMI (Bernstein *et al.* 2012), though initially conceived as a filter to exclude this pixel category in atmospheric correction, can also be used to highlight units corresponding to muddy or marshy spaces:

$$NDMI = \frac{(Red\ edge - NIR2)}{(Red\ edge + NIR2)}$$

Two indices invented to map the presence of iron rich areas, WVII (Worldview Iron Index) and IOR (Iron Oxide Ratio), proved to be effective for Rotzo case study. The former deals with green, yellow and blue bands:

$$WVII = \frac{(Green * Yellow)}{(Blue * 1000)}$$

whereas the latter is the quotient of red and blue band (Segal 1982):

$$IOR = \frac{Red}{Blue}$$

4. Results and discussion

From the analysis of all acquired and processed data, it was possible to identify previously unknown ground anomalies. In order to avoid autocorrelation, we employed the PCA on five different visualizations of the same VHR SfM-derived DEM. The parameters of the SVF and LRM visualizations were set in order to emphasize the morphology of the terrain: for the first, we set a maximum search radius of 1 m and 16 search directions; for the LRM we applied a rectangular low-pass filter with 1 m kernel side. The five derived Principal Components maintain most of the uncorrelated information in the first three of them, leaving in Component four and five most of the noise and only few data. This is the reason why we decided to map Component one, two and three respectively on the red, the green and the blue band. Specifically, we combined hillshade, slope, LRM, SVF and flow direction. This procedure helps to visualize simultaneously much of the variability in the original dataset, providing an informative, global overview for improved photo-interpretation (Fig. 6d).The analysis was carried out by selecting the most informative visualization techniques with the aim of obtaining an overview of the different traces identified on the single treatments.

The observation of the DEM allowed us to identify a polygonal anomaly, composed of two lowered perpendicular lines forming a corner, in the N-E area

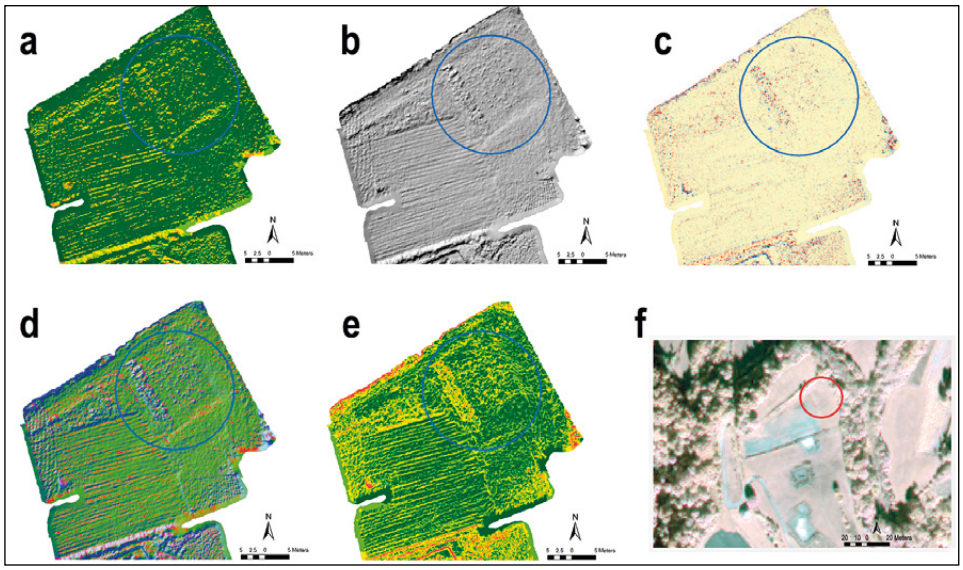

Fig. 6 – North field area, the circles indicate the most significant detected anomalies: a) flow direction analysis; b) hillshade; c) Local Relief Model (LRM); d) PCA of 5 visualization techniques, in particular: flow direction analysis, hillshade, slope analysis, LRM and Sky-View Factor; e) slope analysis; f) multispectral composite bands 7, 3, 2 (Brovey Pansharpening).

of the SfM-derived 3D model. Within this structure, we could also identify a second pseudo-quadrangular anomaly with dimensions comparable to those of the excavated proto-historic houses of the site. Although the two large perpendicular lines are well visible with all visualization techniques (Fig. 6), SVF and LRM (Fig. 6c) proved to be the most effective ones, especially when dealing with small topographic variations. The potential of both techniques to enhance micro-morphologies, confirmed to be particularly useful to highlight even modest anomalies. This evidence, probably related to a pre-roman structure, is located in a private field so it is not possible to open a control trench. However, we conducted a field survey and we were able to locate an *aes rude* and a cluster of ancient, but unfortunately non-diagnostic pottery.

Moreover, we identified two parallel lines in the center of the promontory: they run perpendicular to the slope line and are iso-oriented with structure A on both sides (Fig. 7). The combined use of artificial lighting visualization, such as PCA of 16 hillshades (Fig. 7d), and the flow direction analysis (Fig. 7b) is particularly helpful to identify linear features orthogonal to the slope direction. These structures can be interpreted as remains of ancient terracings related to the construction technique of Raetic villages, as it was seen in other coeval sites, such as Fai della Paganella (Marzatico 1999). Traces of ancient

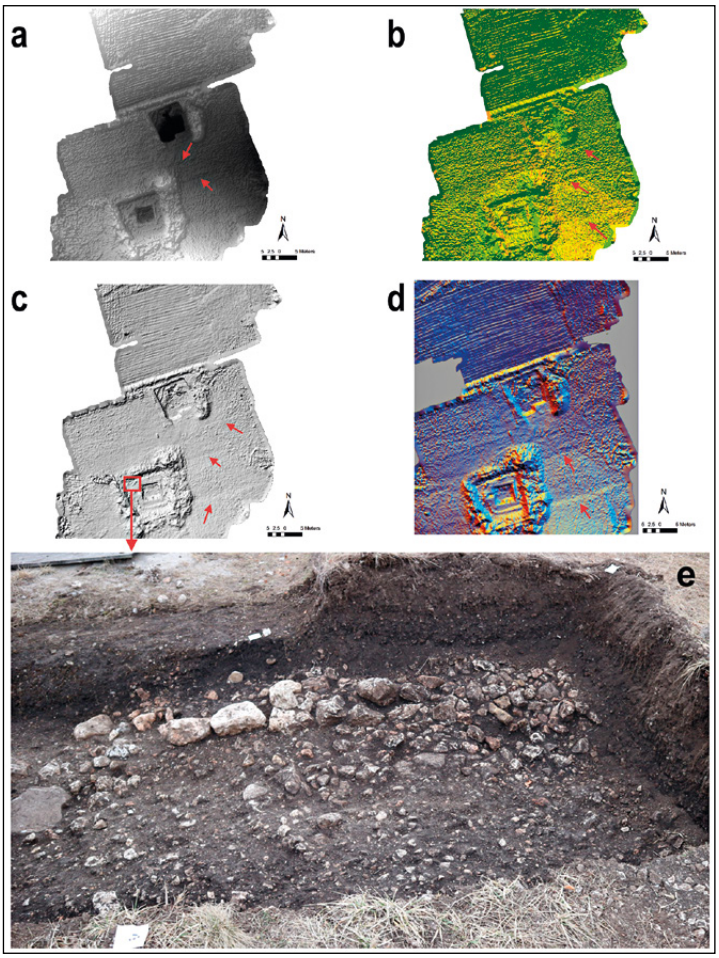

Fig. 7 – Area 1, the arrows indicate the most significant detected anomalies: a) SfM-derived DEM; b) flow direction analysis; c) hillshade; d) PCA of multiple hillshades; e) the ancient wall discovered in correspondence with a linear anomaly north-west of sector A.

terracings were also discovered in Rotzo during the excavations of sectors D and E (De Guio *et al.* 2011; Magnini *et al.* 2017a). A small area on the north-western side of sector A was recently investigated during preventive controls for the construction of a cover of the archaeological structure and revealed the presence of an ancient wall in correspondence with one of the anomalies detected (Fig. 7e). A third linear trace, parallel with the previous ones, was recognized in the middle (and lowest part) of the site (Fig. 7).

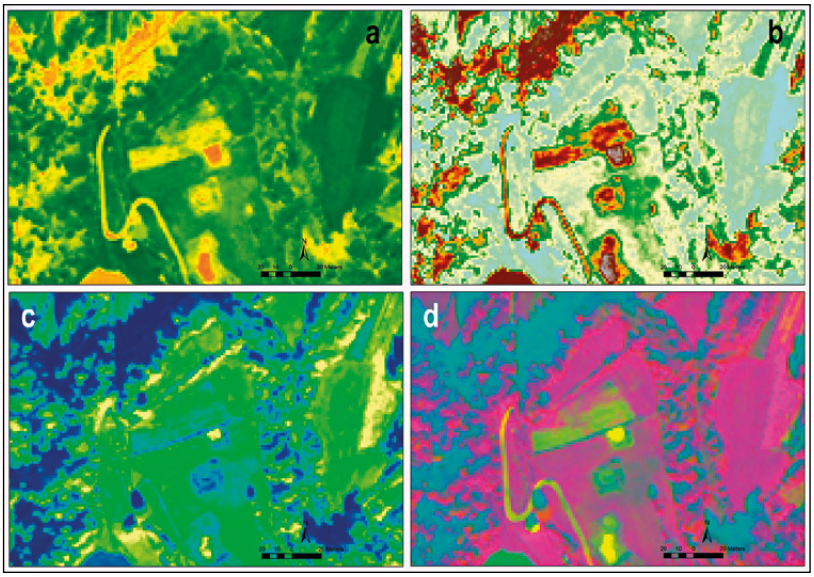

Fig. 8 – Area 1, multispectral image enhancements: a) NDVI; b) WV-VI; c) GNDVI; d) PCA of the 8 multispectral bands.

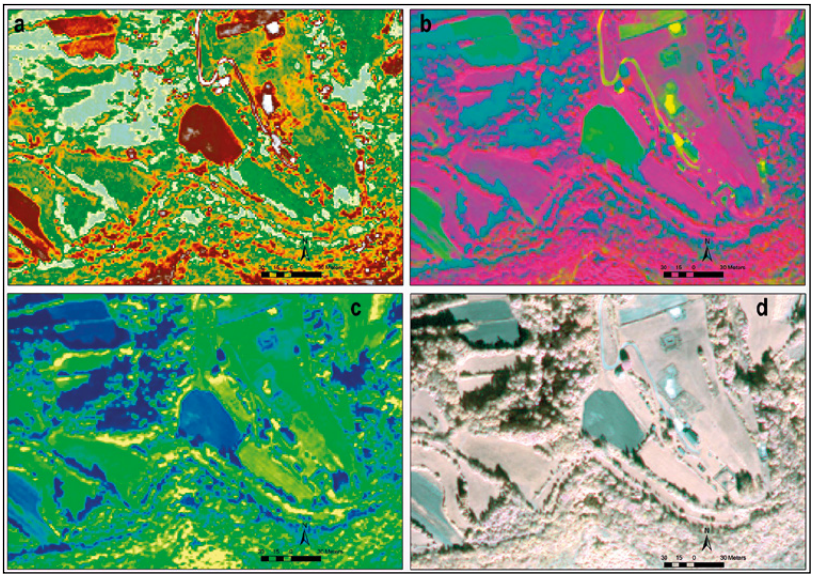

Fig. 9 – Area 2, multispectral image enhancements: a) IOR; b) PCA of the 8 multispectral bands; c) GNDVI; d) multispectral composite bands 7, 3, 2 (Brovey Pansharpening).

Although the nature of this evidence is unclear, it has been suggested that it might refer to a pathway or drainage channel within the site.

All the main features identified on our DEM were also visible on the composite-band multispectral images confirming the presence of terrain anomalies instead of artefacts related to data collection (Fig. 8). The satellite multispectral images showed further interesting traces. The PCA of the 8 bands displays a well-defined trace just next to the excavations of sector D, within a private field (Fig. 8d). This anomaly was also confirmed by the analysis of the Green NDVI (Fig. 8c) that shows an area with a different vegetation growth. This feature is probably connected with the house unit currently under excavation in sector D. In fact, stratigraphic evidence clearly suggests that the same building continues in the direction of the trace.

Fifteen meters E of the sector D, the WorldView Vegetation Index (Fig. 8b) showed a quadrangular feature of about 9 m per side. This trace, as also confirmed by the NDVI (Fig. 8a) and the GNDVI (Fig. 8c), is dimensionally comparable with the houses excavated at Rotzo. The WVVI and the NDVI highlights two other anomalies: the first on the west side of sector D and the second on the E side of the modern road, near the curve. The resolution of the multispectral image does not allow to identify the shapes in detail, but these traces indicate a slight increase in vegetation that may be associated with the presence of buried structures.

The presence of crop-marks and soil-marks in the western private field (area 2) is rather clear in all orthophotos, multispectral data and relative visualizations (Fig. 9). WorldView Iron Index, IOR (Fig. 9a) and PCA (Fig. 9b) of the eight WV bands are some of the most performing image enhancement techniques for identifying those traces. The first, in the north-western corner of the field is a well-defined higher area with dimensions of 20×15 m; the other is a depressed slice of the field measuring approximately 80×15 m located directly on the south side of the previous trace. This evidence shows an irregular outline pattern, if compared to the rest of the field. The area was investigated with a field survey, during which were recovered numerous protohistoric pottery fragments, two glass beads compatible with a Second Iron Age chronology and several metallic (bronze and lead) fragments.

5. Conclusions

The combined use of orthophotos, satellite multispectral imaging, SfM-derived digital elevation models and systematic ground surveys helped us to cross-validate the doubtful anomalies using data from independent sensors and reduced the number of false positives due to the presence of artefact related to data collection. Although the smaller traces can be recognized only on the SfM-derived DEM for its higher spatial resolution, the multispectral

satellite images allowed us to explore a large portion of the electromagnetic spectrum and consequently to identify anomalies which do not correspond to micro-topographical changes at ground-level. Moreover, we could obtain a general overview of the morphology of the Bostel promontory and the surrounding fields, which offered the chance to identify a series of possible archaeological structures in the private areas around the archaeological park. In fact, remote sensing analyses – bridged with fieldwork data – showed a complex environmental model. The houses found during the excavations seem to be embedded in a framework of structures for space organization, defense and territorial control. The existence of a network of terraces and buildings, up to the south-eastern ridge of the Bostel, confirms the existence of an intense human occupation of the entire promontory. All acquired data are contributing to plan the upcoming archaeological excavations and to target future investigations.

This research experience also highlighted the value of the interdisciplinary interaction between archaeologists, remote sensing experts, physicists, aerospace and computer engineers. The creation of the HORUS drone represents a small but significant step in the direction of specialized tools for archaeological aerial prospection and the funding of the follow-up project Horus 2.0 is allowing us to expand the type and resolution of sensors onboard for improved detail and cross-validation potential. In fact, drones represent a fundamental and versatile tool for exploratory surveys and mapping campaigns that offer complete freedom in scheduling month, day and hour of flight (in favorable weather conditions) and multiple campaigns as to select the most appropriate time span for grass/soil/snow/shadow-marks identification in order to monitor the preservation state and transformations of the archaeological heritage.

Luigi Magnini, Cinzia Bettineschi*, Armando De Guio, Laura Burigana
Department of Cultural Heritage: Archaeology, History of Art, Cinema and Music
University of Padova

Giacomo Colombatti, Carlo Bettanini, Alessio Aboudan
Center for Studies and Activities for Space, CISAS "Giuseppe Colombo"
University of Padova

Acknowledgements

Armando De Guio is scientific director of all the investigations on the Bostel since 1993 and of the project Horus 2.0. Cinzia Bettineschi wrote the introduction and the archaeological contextualization of the site. Luigi Magnini worked on SfM, DEM visualizations and discussion of the results. The octocopter chapter is due to Carlo Bettanini, Giacomo Colombatti and Alessio Aboudan. Laura Burigana handled the multispectral data. The conclusions are common to all authors.

* Corresponding author: cinzia.bettineschi@unipd.it

REFERENCES

Benavides López J.A., Aranda Jiménez G., Sánchez Romero M., Alarcón García E., Fernández Martín S., Lozano Medina A., Esquivel Guerrero J.A. 2016, *3D modelling in archaeology: The application of Structure from Motion methods to the study of the megalithic necropolis of Panoria (Granada, Spain)*, «Journal of Archaeological Science: Reports», 10, 495-506.

Bernstein L.S., Jin X., Gregor B., Adler-Golden S. 2012, *Quick atmospheric correction code: Algorithm description and recent upgrades*, «Optical Engineering», 51, 11.

Borie C. 2016, *Mapping on a budget: A low-cost UAV approach for the documentation of prehispanic fields in Atacama (N. Chile)*, «The SAA Archaeological record», 16, 2, 17-21.

Burigana L., Magnini L. 2018, *Image processing and analysis of radar and Lidar data. New discoveries in Verona southern lowland (Italy)*, «STAR: Science & Technology of Archaeological Research», 3, 2, 490-509 (https://doi.org/10.1080/20548923.2018.1426273).

Campana S. 2017, *Drones in archaeology. State-of-the-art and future perspectives*, «Archaeological Prospection», 24, 4, 275-296 (https://doi.org/10.1002/arp.1569).

Challis K., Forlin P., Kincey M. 2011, *A generic toolkit for the visualization of archaeological features on airborne Lidar elevation data*, «Archaeological Prospection», 18, 4, 279-289 (https://doi.org/10.1002/arp.421).

Chavarría Arnau A., Reynolds A. (eds.) 2015, *Detecting and Understanding Historic Landscapes*, Mantova, SAP.

Chiabrando F., Nex F., Piatti D., Rinaudo F. 2011, *UAV and RPV systems for photogrammetric surveys in archaeological areas: Two tests in the Piedmont region (Italy)*, «Journal of Archaeological Science», 38, 3, 697-710.

Colombatti G., Aboudan A., Bettanini C., Magnini L., Bettineschi C., Deotto G., Toninello L., Debei S., De Guio A., Zanovello P., Menegazzi A. 2017, *Korus – A drone project for visual and IR imaging*, in *2017 IEEE International Workshop on Metrology for AeroSpace (MetroAeroSpace)*, 589-592 (https://ieeexplore.ieee.org/document/7999536/).

Colomina I., Molina P. 2014, *Unmanned aerial systems for photogrammetry and remote sensing: A review*, «ISPRS Journal of Photogrammetry and Remote Sensing», 92, 79-97 (https://doi.org/10.1016/j.isprsjprs.2014.02.013).

Crutchley S. 2015, *Using Airborne Lidar for interpreting archaeological landscapes*, in Chavarría Arnau, Reynolds 2015, 67-92.

Dal Pozzo A. 1820 (ris. 1910), *Memorie Istoriche dei Sette Comuni Vicentini*, Bologna.

De Guio A. 2015, *Cropping for a better future. Vegetation indices in archaeology*, in Chavarría Arnau, Reynolds 2015, 109-152.

De Guio A., Bressan C., Ferrari G., Mantoan R., Gamba M., Migliavacca M., Padoan C., Nicosia C. 2011, *Bostel di Rotzo (VI) – stato di avanzamento delle ricerche*, «Quaderni di Archeologia del Veneto», 27, 168-183.

De Reu J., De Smedt P., Herremans D., Van Meirvenne M., Laloo P., De Clercq W. 2013, *On introducing an image-based 3D reconstruction method in archaeological excavation practice*, «Journal of Archaeological Science», 41, 251-262 (https://doi.org/10.1016/j.jas.2013.08.020).

Devereux B.J., Amable G.S., Crow P. 2008, *Visualisation of LIDAR terrain models for archaeological feature detection*, «Antiquity», 82, 470-479.

Estornell J., Martí-Gavliá J.M., Sebastiá T.,Mengual J. 2013, *Principal Component Analysis applied to Remote Sensing*, «Modelling in Science Education and Learning», 6, 83-89.

Fiorillo F., Jiménez Fernández-Palacios B., Remondino F., Barba S. 2013, *3D surveying and modelling of the archaeological area of Paestum, Italy*, «Virtual Archaeology Review», 4, 8, 55-60.

Gillespie A.R., Kahle A.B., Walker R.E. 1986, *Color enhancement of highly correlated images. I. Decorrelation and HSI contrast stretches*, «Remote Sensing of Environment», 20, 209-235.

Green S., Bevan A., Shapland M. 2014, *A comparative assessment of structure from motion methods for archaeological research*, «Journal of Archaeological Science», 46, 173-181 (https://doi.org/10.1016/j.jas.2014.02.030).

He J., Li Y., Zhang K. 2012, *Research of UAV flight planning parameters*, «Positioning», 3, 43-45.

Hesse R. 2010, *LiDAR-derived Local Relief Models – A new tool for archaeological prospection*, «Archaeological Prospection», 17, 2, 67-72 (https://doi.org/10.1002/arp.374).

Hoffer R.M. 1972, *The importance of "ground truth" data in remote sensing*, The Laboratory for Applications of Remote Sensing, Purdue University (https://ntrs.nasa.gov/archive/nasa/casi.ntrs.nasa.gov/19730007768.pdf; accessed December 20, 2017).

Holden N., Horne P., Beweley R.H. 2002, *High-resolution digital airborne mapping and archaeology*, in R. Beweley, W. Raczkowski (eds.), *Aerial Archaeology: Developing Future Practice*, Amsterdam, IOS Press, 173-180.

Jenson S.K., Domingue J.O. 1988, *Extracting Topographic Structure from Digital Elevation Data for Geographic Information System Analysis*, «Photogrammetric Engineering and Remote Sensing», 54, 11, 1593-1600.

Kidd C., Chapman L. 2012, *Derivation of sky-view factors from Lidar data*, «International Journal of Remote Sensing», 33, 11, 3640-3652.

Kokalj Z., Hesse R. 2017, *Airborne Laser Scanning Raster Data Visualization: A Guide to Good Practice*, Ljubljana, Založba ZRC.

Leonardi G. 2010, *Le problematiche connesse ai siti d'altura nel Veneto tra antica età del Bronzo e romanizzazione*, in L. Dal Rì, P. Gamper, H. Steiner (eds.), *Höhensiedlungender Bronze- und Eisenzeit. Kontrolle der Verbindungswege über die Alpen/Abitati dell'età del Bronzo e del Ferro. Controllo delle vie di comunicazione attraverso le Alpi*, Trento, Temi Editrice, 251-276.

Leonardi G., Facchi A., Migliavacca M. 2011, *Una casetta seminterrata dell'età del ferro a Montebello Vicentino*, Vicenza, Italia, «Preistoria Alpina», 45, 243-252.

Leonardi G., Ruta Serafini A. 1981, *L'abitato protostorico del Bostel di Rotzo (Altopiano di Asiago)*, «Preistoria Alpina», 17, 7-75.

Lillesand T.M., Kiefer R.W., Chipman J.W. 2008, *Remote Sensing and Image Interpretation*, Hoboken, Wiley.

Lora S., Ruta Serafini A. 1992, *Il gruppo Magré*, in I.R. Metzger, P. Gleirscher (eds.), *Die Rater/I Reti*, Bolzano, Athesia, 247-272.

Ma Y., Soatto S., Košecká J., Sastry S. 2001, *An Invitation to 3D Vision: From Images to Geometric Models*, Cambridge.

Magnini L., Bettineschi C., De Guio A. 2017a, *Il sito protostorico del Bostel di Rotzo: note di aggiornamento sugli scavi in corso*, in G. Deotto, C. Bettineschi, L. Magnini, L. Toninello (eds.), *Horus, visioni dall'alto dello spazio archeologico. Proceedings of the workshop*, Padova, Padova University Press, 13-19.

Magnini L., Bettineschi C., De Guio A. 2017b, *Object-based shell craters classification from Lidar-derived Sky-View Factor*, «Archaeological Prospection», 24, 211-223.

Magnini L., Bettineschi C. 2019, *Theory and Practice for an object-based approach in archaeological Remote Sensing*, «Journal of Archaeological Science», 107, 10-22 (https://doi.org/10.1016/j.jas.2019.04.005).

Marzatico F. 1999, *L'abitato di Fai della Paganella e i modelli insediativi retici in Trentino*, in R. Poggiani Keller (ed.), *Atti del II Convegno archeologico provinciale (Grosio 1995)*, Sondrio, 151-164.

Marzatico F. 2001, *La seconda età del Ferro*, in M. Lanzinger, F. Marzatico, A. Pedrotti (eds.), *Storia del Trentino*, *I*, *La preistoria e la protostoria*, Bologna, Il Mulino, 479-576.

Migliavacca M. 1994, *La «casa retica» in area veneta*, «Preistoria Alpina», 27, 243-262.

Migliavacca M. 1996, *Lo spazio domestico nell'Età del Ferro, tecnologia edilizia e aree di attività tra VII e I sec. a.C. in una porzione dell'arco alpino orientale*, «Preistoria Alpina», 29, 5-161.

Parcero-Oubiña C., Mañana-Borrazás P., Güimil-Fariña A., Fábrega-Álvarez P., Pino M., Stek T.D. 2016, *Drones over Mediterranean landscapes. The potential of small UAV's (drones) for site detection and heritage management in archaeological survey projects: A case study from Le Pianelle in the Tappino Valley, Molise (Italy)*, «Journal of Cultural Heritage», 22, 1066-1071 (https://doi.org/10.1016/j.culher.2016.06.006).

Pellegrini A. 1915-1916, *La stazione preromana di Rotzo sull'altipiano dei Sette Comuni Vicentini*, «Atti del Reale Istituto Veneto di Scienze, Lettere e Arti», 75, 105-135.

Perini R. 1967, *La casa retica*, «Studi Trentini di Scienze Naturali» Sez. B, 44, 2, 279-297.

Segal D. 1982, *Theoretical basis for differentiation of ferric-iron bearing minerals, using Landsat MSS data*, in *Proceedings of Symposium for Remote Sensing of Environment, 2nd Thematic Conference on Remote Sensing for Exploratory Geology (Fort Worth 1982)*, Ann Arbor (MI), Environmental Research Institute of Michigan, 949-951.

Solano S. 2016, *La romanizzazione in mostra. Di pietra e di legno. Una casa alpina tra età del Ferro e romanizzazione*, in S. Solano (ed.), *Da Camunni a Romani. Archeologia e storia della romanizzazione alpina, Atti del Convegno (Breno - Cividate Camuno 2013)*, Roma, Quasar, 93-134.

Steven M.D. 1987, *Ground truth. An underview*, «International Journal of Remote Sensing», 8, 7, 1033-1038.

Tecchiati U., Rizzi G. 2014, *La "Casa delle botti e delle ruote": scavo di un edificio incendiato del V sec. a.C. nella piana di Rosslauf a Bressanone (BZ)*, in R. Roncador (ed.), *Antichi popoli delle Alpi: sviluppi culturali durante l'età del Ferro nei territori alpini centro-orientali, Atti della giornata di studi internazionali (Sanzeno 2010)*, Trento, Provincia di Trento, 73-103.

Tecchiati U., Sabattoli L. 2011, *Una capanna della recente età del Ferro scavata a Laion, Wasserbuhel (Gimpele) (BZ)*, «Atti dell'Accademia roveretana degli Agiati», 261, ser. IX, vol. I, 91-128.

Verhoeven G. 2011, *Taking computer vision aloft – Archaeological three-dimensional reconstructions from aerial photographs with PhotoScan*, «Archaeological Prospection», 18, 67-73.

Wolf A. 2010, *Using WorldView 2 Vis-NIR MSI Imagery to Support Land Mapping and Feature Extraction Using Normalized Difference Index Ratios*, Longmont, Digital Globe.

Zakšek K., Oštir K., Kokalj Z. 2011, *Sky-view factor as a relief visualization technique*, «Remote Sensing», 3, 398-415.

ABSTRACT

This paper presents the combined use of UAV-derived Digital Elevation Models, optical and IR imaging and multispectral satellite images to produce a (micro)topographic survey of the proto-historic village of Bostel, in the municipality of Rotzo (province of Vicenza, Italy). It aims to improve our knowledge of the structural organization of the site. Different vegetation indices were calculated from the multiband images to enhance the grass and soil-marks in open field, allowing the identification of buried structures. Close-range images were acquired with a commercial DJI Phantom 2 and a customized unmanned aerial vehicle (UAV), equipped with both high-resolution digital and IR cameras. Structure from Motion was used on the acquired data to create digital elevation models (DEM) of sample areas, which were enhanced by using different data visualization techniques. Remote sensing analyses were then combined with fieldwork data, producing a complex environmental model. The houses found during the excavations seem to be embedded in a framework of structures for the sake of space organization, defence and control. Moreover, the presence of a dense network of terraces and buildings, running right up to the south-eastern ridge of the promontory, confirms the existence of an intense human occupation of the entire area.